

# Parameter Identification and Optimization of an Oceanographic Monitoring Remotely Operated Vehicle

Jorge Rojas, Mike Eichhorn  
Institute for System Analysis  
Ilmenau University of Technology  
98693 Ilmenau, Germany  
jorge.rojas@tu-ilmenau.de,  
mike.eichhorn@tu-ilmenau.de

Ganzorig Baatar, Sebastian Matz  
Advanced System Technology (AST)  
Branch of Fraunhofer IOSB  
98693 Ilmenau, Germany  
ganzorig.baatar@iosb-ast.fraunhofer.de,  
sebastian.matz@iosb-ast.fraunhofer.de

Thomas Glotzbach  
Faculty Electrical Engineering &  
Computer Science  
Aalen University  
73430 Aalen, Germany  
thomas.glotzbach@hs-aalen.de

**Abstract**—Remotely operated underwater vehicles (ROV) have become a commonly used platform for many different surveys and the operation of the ROV must be done by highly trained personnel. In order to make the operation of ROVs less complicated and reduce the workload for the operators, it is necessary to have an intelligent control system. The development of an intelligent control system requires an accurate model of an underwater vehicle. However, the necessary parameters within the vehicle model are difficult to determine, especially those concerned with hydrodynamic effects. This paper presents the development of a dynamic and accurate model of an ROV which includes the vehicle motion, gravity, buoyancy effect and the behavior of the vehicle with respect to the forces or moments generated by the thrusters, commanded by the control inputs. An accurate model requires an exact identification of parameters, in order to simulate the real motion of the vehicle. Thus, the main part of this work focuses on hydrodynamic parameter estimation, such as added mass and damping effects, using real underwater motion tests. Due to limitations in the nature of the underwater vehicle not all parameters could be identified. To overcome this problem, an optimization method is performed, which allows to minimize the error between the simulation results and the real motion behavior and thus, to reach an accurate dynamic model of the remotely operated vehicle.

**Index Terms**—Remotely Operated Vehicle, Modeling, Parameter Identification, Hydrodynamic Parameters, Parameter Optimization

## I. INTRODUCTION

Remotely Operated Underwater Vehicles (ROVs) have become a commonly used robotic platform in oceanographic monitoring and analysis. Modern ROVs cover tasks from inspecting the hazardous inside of nuclear power plants to repairing complex deep water production systems offshore for the oil and gas industry [1].

Accuracy of the model is fundamental for successful simulation and controller design. Therefore, is important to study the mathematical representation of the ROV which includes the Kinematics and Kinetics in a state-space (vectorial) repre-



Fig. 1: ROV-BWSTI [10]

sentation proposed by Fossen [2]. This type of representation provides an effective way to model and analyse the ROV.

The parameter estimation process includes empirical methods based on work of Eidsvik and Schjølberg [3] and real underwater tests. Other parameters, such as center of gravity or moments of inertia needed for modeling the ROV-BWSTI are estimated by means of a 3D model of the vehicle. An experimental estimation method for the hydrodynamic parameters was suggested by Eng [4] and Eidsvik [5]. In both of these papers, the authors suggest the comparison of the determined parameters with computational fluid dynamics (CFD) program result, which confirmed the parameter values estimated at experimental trials. In some cases, a mathematical model was established at first and an experimental verification was done with a help of a scale model in a tow tank [6] or with a help of the vehicle itself [7].

Another important part of modeling is to determine the thrust allocation and the behavior of the vehicle with respect to the propellers (relation between the force/moment and the control input signal). This approach was done by Taubert and Eichhorn [8] for an AUV. The thrust characteristic identification in this paper is carried out in each degree of freedom by means of several experimental tests and the later interpolation of the obtained values through direct regression.

The experimental part of the parameter identification pro-

cedure was performed on the ROV-BWSTI (Fig. 1) vehicle, designed by Fraunhofer IOSB-AST Institute in Ilmenau [10]. For the experimental validation and parameter identification, the vehicle was set to the Fraunhofers ROV testing facility [11].

ROV-BWSTI is a high maneuverable remotely operated vehicle capable of fulfilling numerous tasks in the matter of sensing. Compared to other underwater vehicles, it is equipped with an internal energy storage, which allows the communication between the ROV and the control station through a special lightweight optical fiber. The optical fiber causes a minimal drag force during the motion. The internal battery is changeable, which allows to continue the mission with short time interruption as the first battery is drained. This vehicle is equipped with six thrusters to control four degrees of freedom (surge, sway, heave, and yaw). ROV-BWSTI specifications are listed in Table I:

Size (LxWxH):	960 mm x 575 mm x 480 mm
Weight:	61 kg
Maximum diving depth:	60 m
Deployment time:	approx. 4 hours
Fiber optic cable length:	800 m
Battery pack life time:	500 charge cycles
Thrusters:	2 Surge, 2 Sway, 2 Heave
Sensor equipment:	9-DOF AHRS Pressure Sensor, GPS, USBL-Modem, Altimeter, Forward looking Sonar, Forward looking Camera, Water quality sensor, Water sampler system.

TABLE I: ROV-BWSTI Specifications [10]

This paper is organised as follows. Section II discusses the mathematical model of an open frame ROV. Section III provides the parameter estimation process for the ROV-BWSTI vehicle. The model simulation based on MATLAB/Simulink model of the vehicle is presented in Section IV followed by Section V in which the parameter optimization procedure is described. Finally, Sections VI and VII contain conclusion and further work plans.

## II. MATHEMATICAL MODEL

According to Fossen [9], the dynamics of the motion of the ROV considering six degrees of freedom (6 DOF) can be presented in a compact matrix-vector form. It describes the equations that represent the model of the vehicle based on its kinematics and kinetics. This type of representation provides an effective way to model and analyse the ROV.

SNAME Notation [12] is used as standard notation in the motion description. The 6 DOF are defined as *surge*, *sway*,

*heave*, *roll*, *pitch*, *yaw*.

$$\begin{aligned}\eta &= [x \ y \ z \ \phi \ \theta \ \psi]^\top \\ \nu &= [u \ v \ w \ p \ q \ r]^\top \\ \tau &= [X \ Y \ Z \ K \ M \ N]^\top\end{aligned}$$

where  $\eta$  refers to the position and orientation in NED frame,  $\nu$  refers to linear and angular velocities in BODY frame and  $\tau$  represents the vector of forces and moments.

### A. Kinematics

In order to analyse the geometrical aspects of the vehicle motion in an inertial frame, it is necessary to transform vectors through changes in reference frames. Euler Angles Transformation is used to achieve this task, according to Fossen [9]. Two coordinate systems are used to describe the orientation, position and motion of the ROV: North-East-Down frame (NED) and Body frame (BODY).

$$\dot{\eta} = \mathbf{J}(\eta)\nu = \begin{bmatrix} \mathbf{J}_1(\eta) & \mathbf{0} \\ \mathbf{0} & \mathbf{J}_2(\eta) \end{bmatrix} \nu$$

$$\begin{aligned}\mathbf{J}_1(\eta) &= \begin{bmatrix} c\psi c\theta & -s\psi c\phi + c\psi s\theta s\phi & s\psi s\phi + c\psi c\phi s\theta \\ s\psi c\theta & c\psi c\phi + s\phi s\theta s\psi & -c\psi s\phi + s\theta s\psi c\phi \\ -s\theta & c\theta s\phi & c\theta c\phi \end{bmatrix} \\ \mathbf{J}_2(\eta) &= \begin{bmatrix} 1 & s\phi t\theta & c\phi t\theta \\ 0 & c\phi & -s\phi \\ 0 & s\phi/c\theta & c\phi/c\theta \end{bmatrix}\end{aligned}$$

where  $s(\cdot) = \sin(\cdot)$ ,  $c(\cdot) = \cos(\cdot)$ ,  $t(\cdot) = \tan(\cdot)$ .

### B. Kinetics

The analysis of the forces causing the motion of the vehicle is represented in the following equation considering the rigid body kinetics, hydrodynamic and hydrostatic forces.

$$\underbrace{M_{RB}\dot{\nu} + C_{RB}(\nu)\nu}_{\text{rigid-body}} + \underbrace{M_A\dot{\nu}_r + C_A(\nu_r)\nu_r + D(\nu_r)\nu_r}_{\text{hydrodynamic}} + \underbrace{g(\eta)}_{\text{hydrostatic}} = \tau$$

Where:

$M_{RB}$	$\Rightarrow$	Rigid-body inertia matrix
$C_{RB}(\nu)$	$\Rightarrow$	Coriolis-centripetal matrix due to rotation
$g(\eta)$	$\Rightarrow$	Restoring forces vector
$M_A$	$\Rightarrow$	Hydrodynamical added mass matrix
$C_A(\nu_r)$	$\Rightarrow$	Coriolis and centripetal matrix
$D(\nu_r)$	$\Rightarrow$	Hydrodynamic damping matrix
$\nu$	$\Rightarrow$	Generalized velocity vector
$\nu_r$	$\Rightarrow$	Relative velocity vector
$\tau$	$\Rightarrow$	Generalized vector of forces and moments

It is important to mention that  $\nu_r$  describes the relative velocity of the vehicle taking into consideration the effect of environmental disturbances such as ocean currents.

### C. Actuators

The thruster forces and moments defined in the body frame are related to the thruster allocation. It can be represented as [9]:

$$\tau = BKu. \quad (1)$$

$B$  is the thruster configuration matrix which represents the force of each thruster acts in relation to each degree of freedom.  $K$  is the force coefficient matrix which is a function that is determined by thruster force tests and shows the relationship between the force and the input variable (e.g. Force [N] to Input Percentage [%]). Lastly,  $u$  is referred to the control inputs related to each thruster.

### III. PARAMETER ESTIMATION

This section contains the explanation of the parameters estimation required by the mathematical modeling of the ROV in order to validate the real dynamics of the vehicle. One of the problems in the designing of a marine vehicle model is the estimation of the hydrodynamical parameters. Accurate values of parameters ensure proper functioning and improve the performance of model based controllers in real scenarios. Three methods which are used in the estimation and identification of the dynamic and hydrodynamic parameters are briefly described. An Empirical method based on the work of Eidsvik [5] is used to calculate hydrodynamical parameters such as added mass and damping. Rigid body parameters like mass, moments of inertia, center of gravity and allocation of the thrusters are calculated with the help of a 3D Model of the vehicle using Solidworks 3D CAD [13] software. In order to obtain a comparison source for the estimated parameters, a set of experimental tests were performed to the vehicle.

#### A. Empirical Estimation Method

Empirical methods such as Strip Theory and Empirical 3D Data can be used to determine the added mass and damping parameters related to the hydrodynamic effects of the vehicle during the motion. Strip Theory is based on the division of the vehicle in a set of layers or strips. Therefore, two-dimensional hydrodynamical coefficients can be calculated and summarized over the length of the body, which gives the three-dimension hydrodynamical coefficients [2]. Empirical 3D Data considers experimental results of hydrodynamical coefficients of certain solid shapes (e.g. prism, cube, or sphere) which were already calculated. By considering the shape of the vehicle and the projected area, these coefficients can be used in order to apply a correction factor for accurate results. Both methods were used to calculate the added mass and the damping coefficients. These calculation methods were presented by Eidsvik [5].

#### B. Computational Estimation using 3D Model

It is recommended to use a 3D modeling solution to have a virtual prototype of the desired real model. The more accurate information fed into the modeling software (e.g. dimensions, weights, density, among others), the more precise the obtained

model will be. A complete model of the ROV was designed in CAD (Fig. 1), using the exact weight and density of the material of every part, in order to obtain an ideal representation to the real ROV. Rigid body parameters obtained by the CAD model that are required for the mathematical modeling of the ROV are center of gravity, moment of inertia, projected areas and the thruster allocation. Thruster allocation information allows to calculate and model the thruster forces and moments.

#### C. Parameter Estimation by Experimental Tests

Experimental tests allow to identify the vehicle specific parameters with a higher level of accuracy. These tests were performed at the Fraunhofer IOSB-AST underwater vehicle test facility in Ilmenau. Following parameters can be determined experimentally, which are used in the vehicle modeling:

- 1) Rigid body parameters
  - Weight of the vehicle
  - Center of gravity
  - Thrust allocation
- 2) Hydrodynamical parameters
  - Damping coefficients
  - Buoyancy
  - Center of buoyancy
  - Thrust characteristics

Weighing the vehicle at its operational condition gives the real weight parameter. The center of gravity measurement was performed with help of a simple method. A longitudinal bar that crosses under the sectional side of the vehicle allowed to measure the center of gravity (Fig. 2). Once the ROV stays in equilibrium over the bar, the distance between a reference point and the bar is measured.

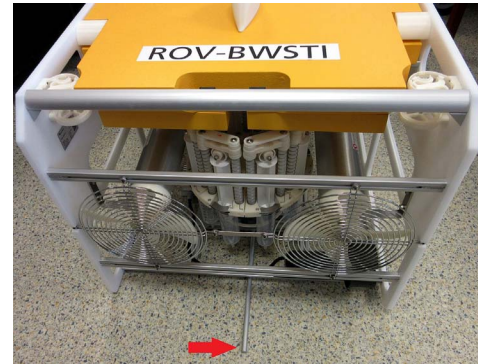


Fig. 2: Center of Gravity estimation

A towing test was performed in order to determine damping coefficients. The ROV, which was mounted to the 3D-Portal (Fig. 3), was driven by it at different constant velocities of 0.05, 0.1, 0.25 and 0.5 m/s. The 3D-Portal is equipped with an force and torque measurement system of ME-Messsysteme Company and monitoring software GSVmulti [14]. The produced damping forces were recorded and interpolated in order to obtain a second order damping curve. So that it is possible to calculate linear and non-linear damping coefficients from this curve.

$$D = c_{const} + c_{lin} * v + c_{quad} * v^2$$

where "D" is the damping force, "c..." are the coefficients of the second order function and "v" is the velocity. In order to avoid surface effects, all tests were conducted at one meter depth and approximately at one meter above the bottom of the basin.

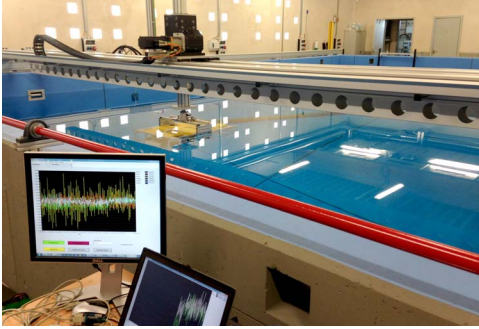


Fig. 3: Towing Test Execution

The following is important to highlight: A mounting profile that maintains the ROV attached to the measuring force system of the 3D-Portal has influences on the damping calculation and should be subtracted from the total damping value.

Figure 4 shows the estimation of the damping coefficients in surge direction. Damping coefficients in sway direction were obtained in the same way. A reliable estimation of the damping parameters in heave direction was not possible. It is observed that the damping force generated by the vehicle at a given velocity cannot reach a constant value as in previous tests in surge and sway direction. Without having certain constant value is it not possible to calculate damping force in this direction.

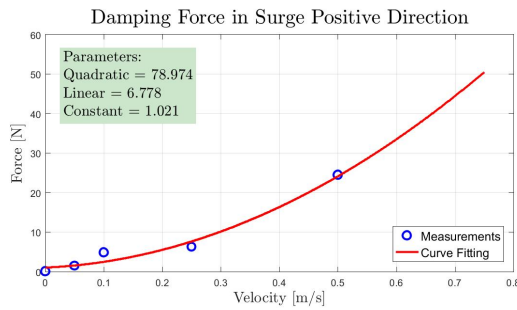


Fig. 4: Damping Force in Surge

In order to determine the buoyancy the vehicle was set into water in its work condition. Additional weights were added until the vehicle can levitate under the water. The extra added weight allows to calculate the force, in which it pulls the vehicle up.

According to Fossen [9] it is possible to state that the center of buoyancy is located vertically on the Z axis, that means

$x_g = x_b$  and  $y_g = y_b$ . Using this statement and applying it in the restoring forces equation of the ROV, this yields:

$$g(\eta) = \begin{bmatrix} (W - B) \sin(\theta) \\ -(W - B) \cos(\theta) \sin(\phi) \\ -(W - B) \cos(\theta) \cos(\phi) \\ -z_b B \cos(\theta) \cos(\phi) \\ -z_b B \sin(\theta) \\ 0 \end{bmatrix}$$

The center of buoyancy on the z axis is computed by using the restoring torques in roll and pitch. It applies a vertical force on the lateral side of the ROV and maintains a fixed pivot where the vehicle will rotate. Then, the tilt angle and the force applied are recorded. It is also necessary to measure the position where the force was applied with respect to the center of gravity (distance  $l$ ), in order to calculate the torque. Figure 5 illustrates the experimental test.

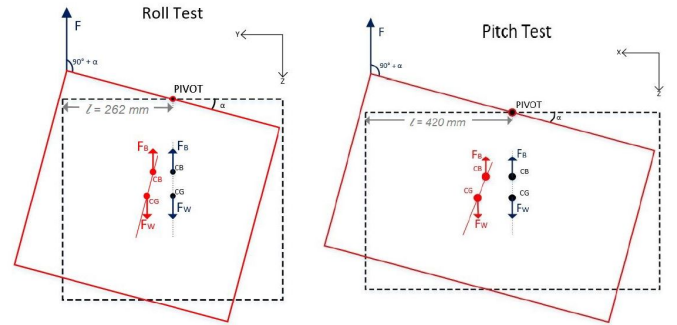


Fig. 5: Diagram of CB Calculation in Roll and Pitch

#### D. Thrust Characteristics

In order to calculate the mapping between the input signal (0 - 100%) and the force [N] or moment [Nm] that acts at the ROV in regards to different degrees of freedom, diverse experimental tests have been made. It is possible to characterize the propeller curves behavior similarly to a non-linear curve of second order polynomial as described in [15], [16] and [17]. The force generated of each degree of freedom on both sides (surge, sway, heave and yaw) is measured at different input signal percentage, in order to formulate and evaluate regression of a quadratic function, and then calculate the characteristic curve that represent the behavior of the propellers force with respect to the input percentage signal.

$$\hat{a}_R = [U_R^T U_R]^{-1} U_R^T y_R$$

$$y_R = \sum_{i=1}^k a_i u_i + \sum_{i=1}^{k-1} \sum_{j=i+1}^k a_{ij} u_i u_j + \sum_{i=1}^k a_{ii} u_i^2$$

The estimated parameters,  $\hat{a}_R$  are calculated in function of an input matrix  $U_R$  and the output  $y_R$  using a model of second order, as shown in the equations above. For this case, the input  $U_R$  is the matrix formed by the set of values of the input signal percentage of the ROV (0% - 100%) and the output  $y_R$  is associated with the force/moment measurements,

both obtained from the thrust experimental trials. The direct regression of the second order model determines the estimate parameters  $\hat{a}_R$ .

$$\hat{a}_R = [a_0 \quad a_1 \quad a_2]$$

$$y_R = a_0 + a_1 u_R + a_2 u_R^2$$

Thrust measurement in surge direction (main thrusters) was accomplished for six different input values. The resulting force curve is shown in figure 6.

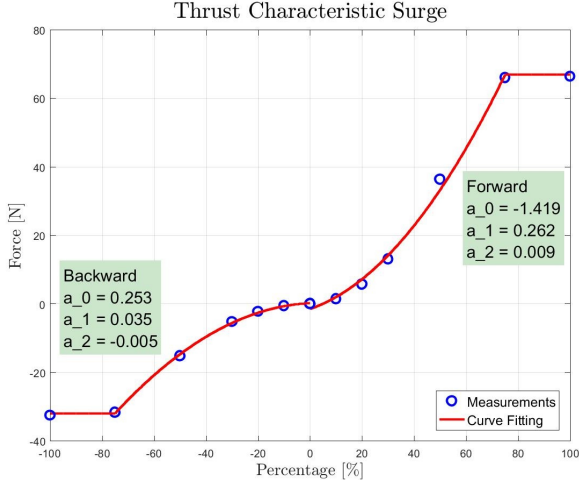


Fig. 6: Thrust Characteristic Curve Surge

As the main thrusters are slightly different from the other remaining thrusters, the force measurement for the sway (Fig. 7) and heave directions, and in yaw rotation was performed at four different input values.

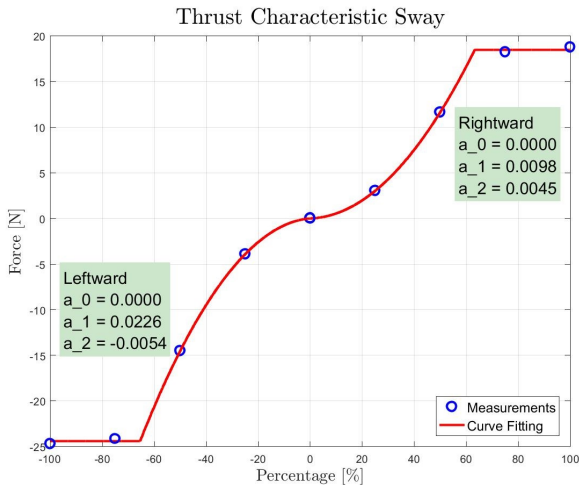


Fig. 7: Thrust Characteristic Curve Sway

Based on the analysis on surge forces, the saturation of the force starts at approximately 70% producing in forward direction 66.35N force and in backward direction 32.56N. This behavior is significant for the open frame ROV, since the main thrusters are mounted on the back of the vehicle.

As seen on the thrust characteristic in sway direction (Fig. 7) the saturation begins between 63% and 67% producing max. 25N force. The rotation of the vehicle is performed by activating the sway thrusters in opposite directions. In this case the torque was measured. The torque value is calculated as the force, produced by the thrusters, is multiplied by the distance of the thrusters from the center of gravity of the vehicle. The torque saturation starts at 65% generating maximal 12Nm.

#### E. Parameter Overview

Parameters obtained using different methods explained above are discussed in this subsection.

1) *Mass*: A 3D Model of the ROV-BWSTI provided a total weight of 59.31kg. The measured weight of the vehicle in operational mode was 61.1kg. For the modeling purpose it is reasonable to use the operational weight of the vehicle.

2) *Moments of Inertia*: Experimental test of moments of inertia calculation was not been performed. Due to the fact that 3D modeling is a suitable approach of the vehicle, parameters obtained from CAD software are used.

3) *Center of Gravity*: The results obtained by using CAD software and results from the real trial, with respect to the center of gravity, are almost the same. These results confirm that the 3D simulation is a fine approximation of the real vehicle. The center of gravity of the experimental trial is used in the modeling.

4) *Damping*: The damping parameter was estimated by empirical and experimental methods, which results are visualized in figures 8 and 9. The damping parameter in heave direction could not be estimated due to certain limitations on the experimental test method. Based on the experimental test results in surge and sway directions, the damping parameter in heave direction can be assumed so that the empirical estimation result would be close to the real parameter.

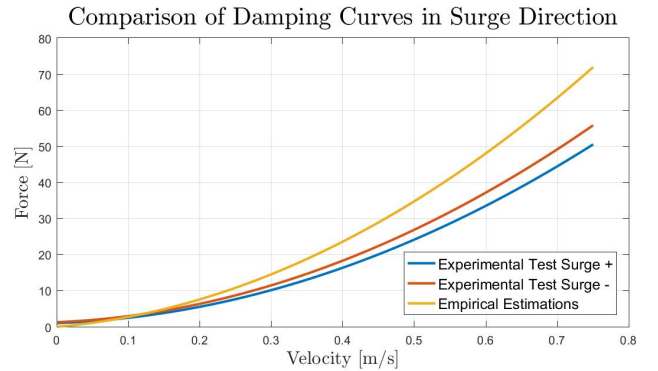


Fig. 8: Damping Results in Surge Direction

5) *Added Mass*: A reliable estimation of the added mass parameters in all degrees of freedom was not possible. Hence, the parameters obtained from empirical estimations are used in the modeling of the ROV and these parameters will be optimized during the acceleration process of the vehicle motion.

6) *Buoyancy*: the experimental estimation explained above gives a result of 294 grams of extra weight. The vehicle buoyancy force results to be 602.31N.

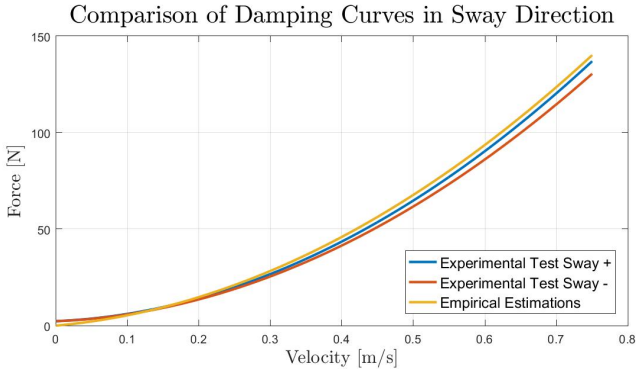


Fig. 9: Damping Results in Sway Direction

7) *Center of Buoyancy*: Similiar to buoyancy, the center of buoyancy estimation procedure was performed experimentally and explained before. The measured results are presented in the following equation:

$$\mathbf{r}_b = [\mathbf{x}_b \quad \mathbf{y}_b \quad \mathbf{z}_b]^T = [0 \quad 0 \quad -0.0625m]^T$$

8) *Thrust identification*: The thruster behavior in all degrees of freedom were estimated experimentally. The analysis and calculation of the relation force/moment with respect to the control input were detailed before.

All the parameters required for the modeling of the ROV are listed in table II in the appendix. They are used in the simulation of the ROV, that is discussed in the next section. Empirical methods show good accuracy considering the shape of the ROV. It is important to point out that a optimization stage based on real motion trials will be performed ahead in order to validate the obtained parameters.

#### IV. MODEL SIMULATION

The mathematical model of the ROV is implemented in MATLAB/Simulink. It considers all the explanation about the dynamics of motion of the ROV mentioned in the mathematical model. It considers as well as all parameters were obtained in the parameter estimation. The model simulation provides a virtual platform where the behavior of the vehicle can be tested. It is also the basis for the later development of the control system design. Figure 10 represents the block diagram used in the design of the vehicle simulation, it contains three main blocks: Actuators, Kinetics and Kinematics.

##### A. Open Loop Simulations

In order to validate and verify the performance of the ROV Simulink model, a set of open loop simulations were performed.

At first, the simulation in surge direction was performed. It assumes that the vehicle is at one meter depth and ocean currents are not considered. The generated force for an input value of 33% in surge direction is  $13.5N$ . This value is consistent with the thrust characteristic identification made before.

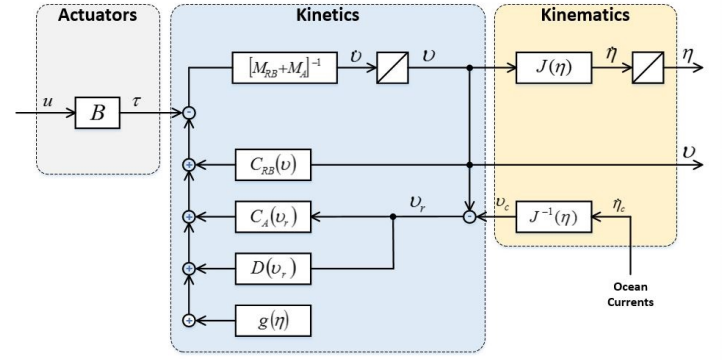


Fig. 10: Block Diagram of the Simulation Model [16]

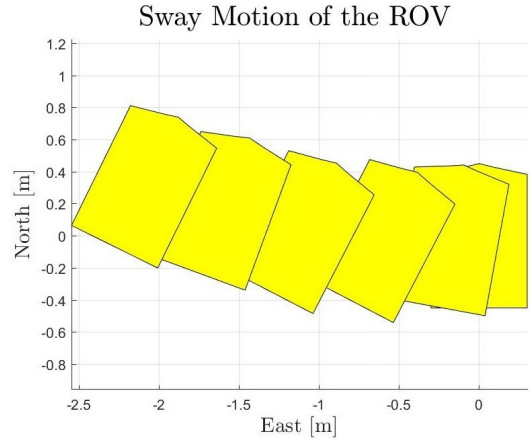


Fig. 11: Sway motion simulation

Similar to the surge direction simulation, a sway motion simulation is performed at one meter depth without ocean currents. At 33% input value for bow and stern propellers generate  $6.62N$  force. A slip angle in the sway motion is observed. This was caused by the position of the side thrusters in the ROV-BWSTI. As the thrusters positioned equidistant to the center of gravity, when the thrusters generate force in the same direction, it generates a rotation moment to the vehicle (Fig. 11). The generated torque was calculated as  $0.57Nm$ .

Heave simulation was performed as the vehicle was submerged with 33% input signal. The force generated by the vertical propellers was approximately  $6.80N$ , which is also consistent in comparison with the measured thrust characteristics.

Yaw rotation is generated by means of bow and stern thrusters, which are used to generate force in sway direction. As described before, the thrusters position are not symmetrical. Therefore, the torque in positive and negative rotations are not equal, which causes drift of the vehicle in sway direction with  $-0.7N$  force. A maximum torque of  $2.50Nm$  was measured by the simulation.

Based on the MATLAB/Simulink model, it is possible to state that the open loop behavior agrees with the real behavior

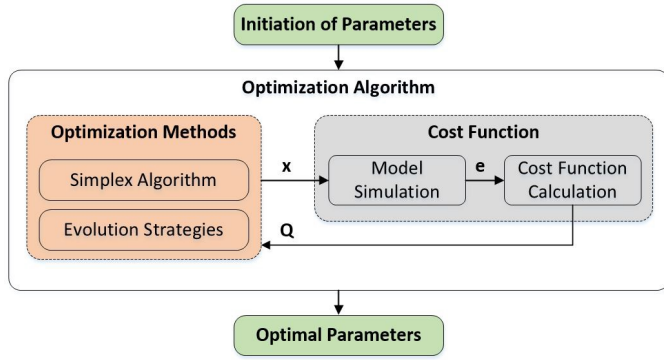


Fig. 12: Parameter Optimization Diagram [16]

of the ROV-BWSTI.

## V. PARAMETER OPTIMIZATION

In order to validate the simulation model, the behavior of the real ROV was identified at different trials. Experimental trials were made under same condition, as described in the model simulation section before. In surge direction, the ROV traveled a distance of 8.6 meters in approximately 25 seconds in the simulation for a given input signal. Using the same input signal the real vehicle covered 7.4 meter distance at the same time. In order to reduce these kind of errors, the optimization of the parameters of the ROV model is performed. This procedure considers the work done by Taubert [16] as a reference. The optimization is performed in four steps. First step is to initialize the parameters that will be optimized and define the boundaries of each parameter. The value boundaries specify the limits of optimization. The parameter obtained in the parameter estimation section (Table II in the appendix) are used as initial values. Data provided by the experimental trials used as a reference in the calculation of error between the simulated data and the real motion data. Second step is the analysis of the quality of the current simulation model. This factor is established as the objective function in the optimization and is evaluated by means of Least Absolute Deviations (LAD) optimality criterion:

$$Q = \int |y(t) - \hat{y}(t)| dt = \int |e(t)| dt$$

The optimization algorithm identifies the global optimum due to use of an evolution strategy algorithm and it computes the optimal parameter in every iteration. To speed up the search process the simplex algorithm is used. Since this algorithm requires a considerable computational effort, it is possible to use the MATLAB Parallel Computing Toolbox (Mathworks, MATLAB/Simulink 2016a) to reduce the convergence time and the computational effort.

The optimization algorithm runs also the simulation in each iteration, seeking for optimized parameters that decrease the error between the reference and the simulated data. For the added mass parameter, the optimization was performed at the first stage of the motion, where the ROV is still accelerating. If



Fig. 13: Surge motion test

the velocity tends to be constant, the damping parameters are optimized. This step is the third stage of the optimization. The last stage evaluates the optimal parameters obtained previously. Figure 12 shows the optimization process principle as described before.

### A. Optimization in Surge direction

Several trials at three different control input signals (33%, 66%, 100%) were performed in order to analyse the motion of the ROV in surge direction. The time and distance were recorded at four different points of the path, as seen in Figure 13. All the trials were performed at one meter depth.

The information recorded on surge trials are used to calculate the objective function in the optimization process. The parameters considered in surge direction for optimization are:

- $X_{\dot{u}}$  : Surge Added Mass Coefficient
- $X_u$  : Surge Linear Damping Coefficient
- $X_{u|u|}$  : Surge Non-linear Damping Coefficient

The force involved in surge motion is the surge force  $\mathbf{X}$ . Therefore, only this input is used in the optimization in order to avoid coupling effects. Figure 14 presents the motion of the ROV in surge direction using the parameters obtained in the optimization for an input signal of 33% and 66%. The green dashed line presents the simulation before the optimization and the yellow line presents the final simulation after the optimization. The circles illustrate the set of the surge trials. As it was discussed before, the force saturation begin at 70% input value. For this reason, a 100% input signal trial delivered almost the same result as 66% input signal trial.

### B. Optimization in Heave Direction

Based on information of the depth sensors, three trials were performed in the optimization of heave parameters by means of the rising up behaviour of the vehicle (Fig. 15). For this test, the vehicle was positioned on the bottom of the basin. No control inputs were involved during the rise of the vehicle which is why the optimization process considers only the buoyancy parameter.

Following parameters were considered in this optimization:

- $Z_{\dot{w}}$  : Added Mass Coefficient in Heave
- $Z_w$  : Linear Damping Coefficient in Heave
- $Z_{w|w|}$  : Non-linear Damping Coefficient in Heave
- $B_s$  : Buoyancy

Figure 16 illustrates the results of the optimization in heave direction. The green dashed line presents the simulation before optimization and the black line presents the final simulation after the optimization. Blue, red and yellow lines describe the heave trials.

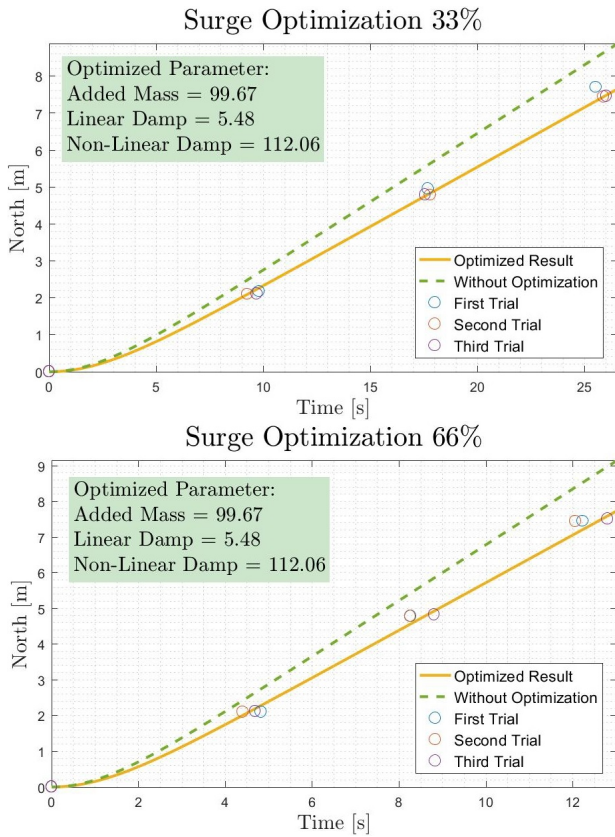


Fig. 14: Optimization results of Surge Motion

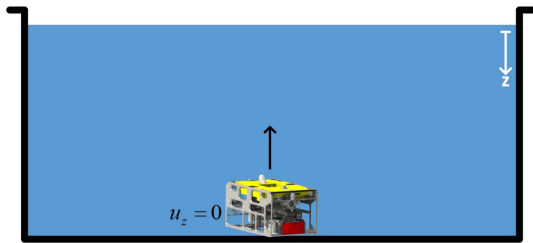


Fig. 15: Rising test

### C. Optimization in Yaw Rotation

Yaw trials were performed by recording five points during the rotation of the vehicle in two laps. The time was recorded at each  $180^\circ$  of rotation. This information is used to calculate the error between the simulated data and the real data.

Results obtained in the optimization of the parameters related to yaw rotation are shown in figure 17. The green dashed line represents the simulation before the optimization and the yellow line represents the final simulation after the optimization. The circles illustrate the set of yaw trials.

### D. Optimization in Sway Direction

The motion of the vehicle in sway direction has a slip angle as discussed before in section IV. The same behavior was recognized in experimental tests. Due to the complexity of the

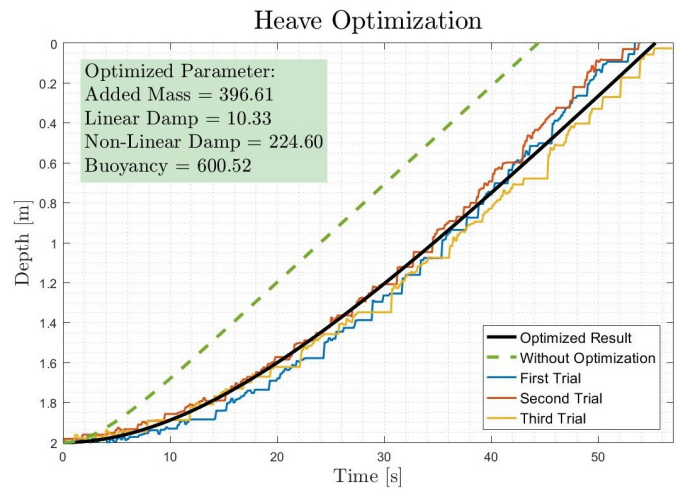


Fig. 16: Optimization results of Heave Motion

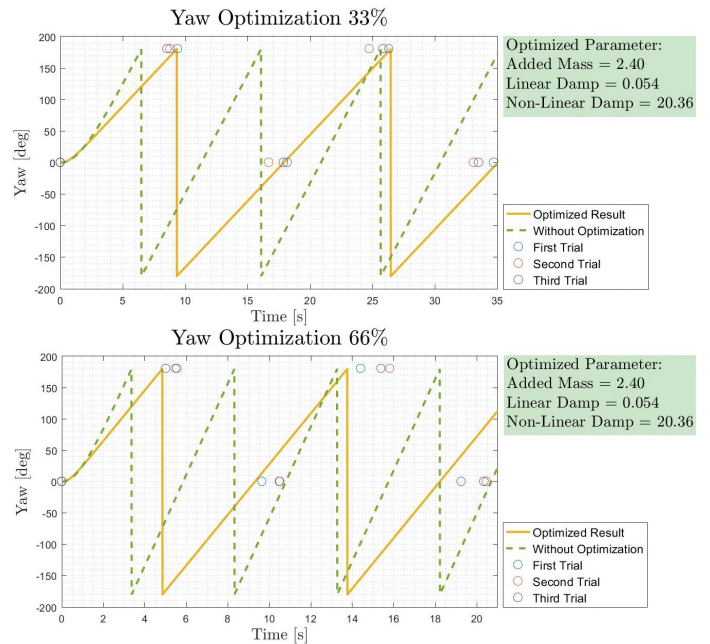


Fig. 17: Optimization results of Yaw Rotation

side effects in sway direction a reference value-set estimation was not feasible.

In this section the optimization of parameters has been performed based on real motion tests of the ROV. It considered the hydrodynamic parameters associated with the motion trials of the vehicle in surge, heave and yaw rotation. Due to the construction feature of the ROV-BWSIT, experimental trials for roll and pitch behavior estimation was not feasible. The optimization process simulates a real motion of the ROV where all the parameters are involved, and calculates the best set of parameters. Table III in the appendix presents the parameters obtained from the optimization phase.

## VI. CONCLUSION

The aim of this work was focused mainly on the identification and optimization of the parameters, required to obtain an accurate model of the ROV-BWSTI. Rigid body and hydrodynamical parameters were obtained using empirical estimation, experimental identification and computational methods. Empirical methods were used for the calculation of hydrodynamic parameters at first. In order to compare the results, experimental tests were performed. The experimentally obtained hydrodynamic parameters proved that empirical estimations are consistent.

A set of parameters required in the mathematical modeling of the ROV. Rigid body and hydrodynamical parameters were obtained using empirical estimations, experimental identification and computational methods. Empirical method used for the calculation of hydrodynamic parameters as a first step. In order to compare the results, experimental tests were performed. Hydrodynamic parameters were obtained also during these experimental tests. This procedure has shown the empirical estimations are in certain degree consistent. Due to limitations on equipment and methods added mass values could not be estimated by experimental tests.

An important part in the modeling is to determine the thrust allocation and the behavior of the thrusters. The thrust characteristic identification was carried out in each degree of freedom by means of several experimental tests and interpolating the obtained values through direct regression.

In order to compare the mathematical model of the ROV with real tests, a modular simulation model in MATLAB/Simulink was developed. It contains in detail all the specifications of the mathematical model. Open loop tests were performed in order to compare the coherent behavior of the simulation.

Since not all the parameters were experimentally identified and compared with the empirical estimations, an optimization stage was performed in order to validate the calculated parameters. After the optimization process, all the required parameters for the modeling were adequately obtained (Table III in the appendix). The optimization process has reduced the error between the real motion tests and the simulation tests in 85.78% for surge motion, 87.91% for heave motion and 75.52% for yaw rotation.

As a result of this work an accurate model of the ROV-BWSTI was successfully obtained which made it possible to start with the first steps of the control system design.

## VII. FURTHER WORK

During the execution of the ROV modeling, the umbilical drag force was not considered. Therefore, the modeling of the umbilical drag force remains to be determined. In order to obtain more accurate hydrodynamic parameters, it is recommended to perform diverse underwater tests and replicate these. In the same way, an increase of the accuracy of the model is possible by rising the number of experimental trials and perform optimization algorithms.

## REFERENCES

- [1] Marine Technology Society - Remotely Operated Vehicles Committee. <http://www.rov.org>
- [2] Fossen, T. I. (1994). *Guidance and Control of Ocean Vehicles*. John Wiley & Sons Inc.
- [3] Eidsvik, O. A. and Schjlberg (2016). Determination of Hydrodynamic Parameters for Remotely Operated Vehicles. ASME 2016 35th International Conference on Ocean, Offshore and Arctic Engineering, 7.
- [4] Eng YH, Lau WS, Low E., Seet GGL and CS Chin, "Estimation of the hydrodynamics coefficients of an ROV using Free Decay Pendulum Motion", *Engineering Letters* 16:329-342, August 2008
- [5] Eidsvik, O. A. (2015). Identification of Hydrodynamic Parameters for Remotely Operated Vehicles. Masters thesis, NTNU.
- [6] Cheng Chin and Michael Lau, "Modeling and testing of hydrodynamic damping model for a complex-shaped Remotely-operated Vehicle for control", *Journal of Marine Science and Application* (2012) 11: 150-163, 2012
- [7] R.Yang, B.Clement, A.Mansour, H.J. Li, M. Li and N.L. Wu, "Modeling of a complex-shaped underwater vehicle", 2014 IEEE International Conference on Autonomous Robot Systems and Competitions (ICARSC), Espinho, Portugal, 2014
- [8] Ralf Taubert, Mike Eichhorn, Christoph Ament, Marco Jacobi, Divas Karimanzira and Torsten Pfuetznerreuter, "Model identification and controller parameter optimization for an autopilot design for autonomous underwater vehicles", *Oceans 2014 - Taipei*, April 2014
- [9] Fossen, T. I. (2011). *Handbook of Marine Craft Hydrodynamics and Motion Control*.
- [10] ROV Familie. Fraunhofer ISOB-AST. <https://www.iosb.fraunhofer.de/servlet/is/5969/>
- [11] Wasser und Mobile Systeme. Fraunhofer ISOB-AST. <https://www.iosb.fraunhofer.de/servlet/is/14961/>.
- [12] SNAME (1950). *Nomenclature for treating the motion of a submerged body through a fluid*. Society of Naval Architects and Marine Engineers
- [13] Dassault Systems SolidWorks Corp.. <https://www.solidworks.com>
- [14] ME Messsysteme GmbH Sensor's Company. <https://www.me-systeme.de/en>, Last accessed on Jun. 21, 2017.
- [15] Fossen, T. I. (2002). *Marine Control Systems: Guidance, Navigation and Control of Ships, Rigs and Underwater Vehicles*.
- [16] Taubert, R. (2014). *Entwicklung und Implementierung von Algorithmen zur Modellidentifikation und zur Unterstützung beim automatischen Reglerentwurf fuer autonome Unterwasserfahrzeuge*. Masterarbeit, Technische Universitaet Ilmenau.
- [17] Glotzbach, T. and Eichhorn, M. (2017). Lecture notes in System Identification Laboratory Session "Design of experiments".

APPENDIX

Parameter Description	Notation	Value	Unit
Mass	$m$	61.10	[kg]
Moment of Inertia Surge	$I_x$	2.45	[kg.m <sup>2</sup> ]
Moment of Inertia Sway	$I_y$	5.60	[kg.m <sup>2</sup> ]
Moment of Inertia Heave	$I_z$	5.60	[kg.m <sup>2</sup> ]
Center of Gravity	$r_g$	$[0 \ 0 \ 0]^T$	[m]
Center of Buoyancy	$r_g$	$[0 \ 0 \ -0.06]^T$	[m]
Buoyancy	$B$	602.33	[N]
Added Mass Coeff. Surge	$X_{\dot{u}}$	65.49	[kg]
Added Mass Coeff. Sway	$Y_{\dot{v}}$	148.24	[kg]
Added Mass Coeff. Heave	$Z_{\dot{w}}$	183.66	[kg]
Added Mass Coeff. Roll	$K_{\dot{p}}$	1.52	[kg.m <sup>2</sup> ]
Added Mass Coeff. Pitch	$M_{\dot{q}}$	5.17	[kg.m <sup>2</sup> ]
Added Mass Coeff. Yaw	$N_{\dot{r}}$	4.63	[kg.m <sup>2</sup> ]
Linear Damping Coeff. Surge	$X_u$	6.78	[kg/s]
Linear Damping Coeff. Sway	$Y_v$	15.88	[kg/s]
Linear Damping Coeff. Heave	$Z_w$	45.84	[kg/s]
Linear Damping Coeff. Roll	$K_p$	0.09	[kg.m <sup>2</sup> /s]
Linear Damping Coeff. Pitch	$M_q$	0.16	[kg.m <sup>2</sup> /s]
Linear Damping Coeff. Yaw	$N_r$	0.13	[kg.m <sup>2</sup> /s]
Non-linear Damping Coeff. Surge	$X_{u u }$	78.97	[kg/m]
Non-linear Damping Coeff. Sway	$Y_{v v }$	218.22	[kg/m]
Non-linear Damping Coeff. Heave	$Z_{w w }$	286.51	[kg/m]
Non-linear Damping Coeff. Roll	$K_{p p }$	1.85	[kg.m <sup>2</sup> ]
Non-linear Damping Coeff. Pitch	$M_{q q }$	7.82	[kg.m <sup>2</sup> ]
Non-linear Damping Coeff. Yaw	$N_{r r }$	6.20	[kg.m <sup>2</sup> ]

TABLE II: Required Parameters for ROV Modelling.

Description	Parameters		Estimated	Optimized
	Notation	Unit		
Added Mass (Surge)	$X_{\dot{u}}$	[kg]	65.49	<b>99.67</b>
Linear Damping (Surge)	$X_u$	[kg/s]	6.78	<b>5.48</b>
Non-linear Damping (Surge)	$X_{u u }$	[kg/m]	78.97	<b>112.06</b>
Least Absolute Error (Surge)	$Q_X$	—	22.64	<b>3.22</b>
Added Mass (Heave)	$Z_{\dot{w}}$	[kg]	183.66	<b>396.61</b>
Linear Damping (Heave)	$Z_w$	[kg/s]	45.84	<b>10.33</b>
Non-linear Damping (Heave)	$Z_{w w }$	[kg/m]	286.51	<b>224.60</b>
Buoyancy	$B$	[N]	602.33	<b>600.52</b>
Least Absolute Error (Heave)	$Q_Z$	—	6777.21	<b>819.62</b>
Added Mass (Yaw)	$N_{\dot{r}}$	[kg.m <sup>2</sup> ]	4.63	<b>2.40</b>
Linear Damping (Yaw)	$N_r$	[kg.m <sup>2</sup> /s]	0.13	<b>0.05</b>
Non-linear Damping (Yaw)	$N_{r r }$	[kg.m <sup>2</sup> ]	6.20	<b>20.36</b>
Least Absolute Error Yaw	$Q_\Psi$	—	59.26	<b>14.51</b>

TABLE III: Estimated and Optimized Parameters.